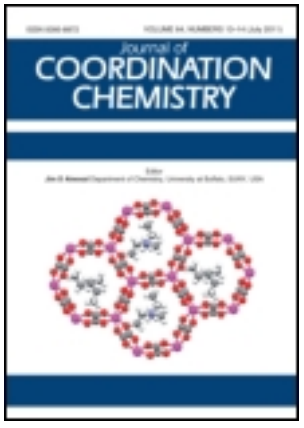


Journal of Coordination Chemistry
Publication details, including instructions for authors and subscription information:
http://www.tandfonline.com/loi/gcoo20

# Hydrothermal syntheses, crystal structures, and properties of two new organic-inorganic hybrid compounds based on polyoxometalates and pyridyl imidazole

Jiuyu Guo [a] , Xiaofei Jin [b] , Lei Chen [a] , Zuoxiang Wang [b] & Yan Xu [a]

[a] College of Chemistry and Chemical Engineering, State Key Laboratory of Materials-Oriented Chemical Engineering, Nanjing University of Technology , Nanjing 210009 , P.R. China
[b] School of Chemistry and Engineering, Southeast University , Nanjing 211189 , P.R. China
Accepted author version posted online: 03 Sep 2012.Published online: 18 Sep 2012.

To cite this article: Jiuyu Guo , Xiaofei Jin , Lei Chen , Zuoxiang Wang & Yan Xu (2012) Hydrothermal syntheses, crystal structures, and properties of two new organic-inorganic hybrid compounds based on polyoxometalates and pyridyl imidazole, Journal of Coordination Chemistry, 65:21, 3821-3832, DOI: 10.1080/00958972.2012.725847

To link to this article: http://dx.doi.org/10.1080/00958972.2012.725847

*Journal of Coordination Chemistry*
Vol. 65, No. 21, 10 November 2012, 3821–3832



# Hydrothermal syntheses, crystal structures, and properties of two new organic–inorganic hybrid compounds based on polyoxometalates and pyridyl imidazole

JIUYU GUO†, XIAOFEI JIN‡, LEI CHEN†, ZUOXIANG WANG‡ and YAN XU*†

†College of Chemistry and Chemical Engineering, State Key Laboratory of Materials-Oriented Chemical Engineering, Nanjing University of Technology, Nanjing 210009, P.R. China
‡School of Chemistry and Engineering, Southeast University, Nanjing 211189, P.R. China

(*Received 1 June 2012; in final form 10 August 2012*)

Two new organic–inorganic hybrid compounds based on polyoxometalates (POMs) and pyridyl imidazole, $[Co(pyim)_3][HPW_{12}O_{40}]\cdot 4H_2O$ (**1**) and $[Ni(pyim)_3]_2[PMo^{V}Mo^{VI}_{11}O_{40}]\cdot 1.5H_2O$ (**2**) (pyim = 2-(2-pyridyl)-imidazole), have been hydrothermally synthesized. The structures of **1** and **2** were determined by single-crystal XRD. Other characterizations were performed by thermogravimetric, infrared spectra, and ultraviolet excitation and emission spectra. Interestingly, $(H_2O)_4$ clusters exist in the structure of **1**, which connect organic ligands by hydrogen bonds to sheets, while connecting POMs to other sheets, thus forming the supramolecular sandwich structure by inorganic layer and organic layer spaced at intervals. In the structure of **2**, two $[PMo^{V}Mo^{VI}_{11}O_{40}]^{4-}$ anions connect by the van der Waals force, then the dipolymers are further linked by $[Ni(pyim)_3]^{2+}$ by hydrogen bonds to form the supermolecular structure.

*Keywords*: Polyoxometalate; Organic–inorganic hybrid; Crystal structure; Hydrogen bond; Water cluster



## 1. Introduction

Organic–inorganic hybrid materials have diverse structures, interesting topological frameworks, and potential properties with applications in catalysis, magnetism, medicine, biology, and materials science [1–10]. Polyoxometalates (POMs) have been used to construct inorganic–organic hybrid frameworks due to their high-negative charges, diverse structures, and nucleophilic oxygen-enriched surface [11–29]. Hybrid compounds based on POMs and heterocyclic species have been reported, such as $(Hpbpy)_5[PW_{11}O_{39}Co(pbpy)]\cdot 2H_2O$ (pbpy = 5-phenyl-2-(4-pyridinyl)-pyridine) [13], $[Co(HPO_3)_2(C_{12}H_8N_2)_8(H_2O)](H_3O)[PW^{VI}_9V^{IV}_3O_{40}(V^{IV}O)_2]\cdot H_2O$ [14], $\{[Co(dpdo)_3]_4(PMo_{12}O_{40})_3[H(H_2O)_{28}(CH_3CN)_{12}]\}_n$ (dpdo = 4,4′-bipyridine-*N*,*N*′-dioxide) [15],

*Corresponding author. Email: yanxu@njut.edu.cn


ISSN 0095-8972 print/ISSN 1029-0389 online 
http://dx.doi.org/10.1080/00958972.2012.725847

$[Mn(2,2'\text{-bipy})_3]H_2[Mn(2,2'\text{-bipy})_2][P_2W_{18}O_{62}]$ and $[Co(H_2biim)_3)]_2H_2[P_2W_{18}O_{62}]\cdot 8H_2O$ (2,2′-bipy = 2,2′-bipyridine, $H_2biim$ = 2,2′-biimidazole) [16], $[Co(2,2'\text{-bipy})_3][\alpha\text{-}H_5PW_{11}CoO_{40}]\cdot 3H_2O$ and $[Fe(2,2'\text{-bipy})_3]_2[\alpha\text{-}HBW_{12}O_{40}]\cdot 2.5H_2O$ [17], $[Cu^I_5Cu^{II}_3(ptz)_8(H_2O)][HSiW_{12}O_{40}]$, $[Cu^I_{10}Cu^{II}_2(ptz)_8(Cl)_3][PW_{12}O_{40}]$, and $[Cu^I_2Cu^{II}_5(ptz)_6][PMo^V_3Mo^{VI}_9O_{40}]\cdot 8H_2O$ (ptz = 5-(2-pyridyl)-tetrazole) [18], and $[Ni_7(H_2O)_6(L)_2(O)_2](Cl)_2(NO_3)_2\cdot 6(H_2O)\cdot(Emim)_2$ ($H_4L$ = 4,4′,4″,4‴-(2,2′,2″,2‴-(ethane-1,2diylbis(azanetriyl))-tetrakis-(methylene)-tetrakis (1H-benzo[*d*]imidazole2,1-diyl))-tetrakis(methylene)-tetrabenzoic acid, [Emim]Cl = 1-ethyl-3-methylimidazolium chloride) [19]. Pyridyl imidazoles and their derivatives have attracted attention for their frameworks and potential properties. Several complexes have been synthesized based on transition metals and pyridyl imidazoles, such as $Ni(L)_2(CNS)_2$ (L = 2-(2′-pyridyl)-imidazole) [20], $PPh_4[Cr(pyim)(C_2O_4)_2]\cdot H_2O$ (pyim = 2-(2′-pyridyl)-imidazole, $C_2O_4^{2-}$ = dianion of oxalic acid, $PPh_4^+$ = tetraphenylphosphonium cation) [21], $[Mn(pyim)_2(N_3)_2]$ [22], $[Cu(H_2bim)(NCS)_2]_n$ ($H_2bim$ = 2,2′-biimidazole) [23], $[Mn(pyim)_2(C_5O_5)]$ ($C_5O_5^{2-}$ = croconate (dianion of 4,5-dihydroxy-4-cyclopentene-1,2,3-trione) [24], $NH_4[OV(O_2)_2\{2\text{-}(2'\text{-pyridyl})\text{-imidazole}\}]\cdot 4H_2O$ [25], $[Zn_2(OH)(pyim)(BIPA)]_n$ ($H_2BIPA$ = 5bromoisophthalic acid) [26], $Zn(L)_2H_2O$ (HL = 2-(2-pyridyl)-benzimidazole) [27], and $[Zn(L)(oba)]$ (L = 2-(2-pyridyl)-imidazole, $H_2oba$ = 4,4′-oxydibenzoic acid) [28]. Although many complexes containing transition metals and pyridyl imidazoles have been prepared, hybrid materials constructed from POMs and pyridyl imidazoles were rarely reported [29]. We therefore design hybrid POMs-pyim in order to explore their properties and understand the formation mechanism. In this article, we hydrothermally prepare two new hybrid compounds, $[Co(pyim)_3][HPW_{12}O_{40}]\cdot 4H_2O$ (**1**) and $[Ni(pyim)_3]_2[PMo^VMo^{VI}_{11}O_{40}]\cdot 1.5H_2O$ (**2**), by using Keggin structure POMs and 2-(2-pyridyl)-imidazole. In the structure of **1**, $(H_2O)_4$ water clusters connect $[HPW_{12}O_{40}]^{2-}$ and $[Co(pyim)_3]^{2+}$ to form inorganic sheet-like and organic sheet-like structures. In **2**, two $[PMo^VMo^{VI}_{11}O_{40}]^{4-}$ anions are connected by the van der Waals force to form a "dipolymer," which was further connected by $[Ni(pyim)_3]^{2+}$ to form the supermolecular framework.

## 2. Experimental

### 2.1. *Materials and physical techniques*

2-(2-Pyridyl)-imidazole was prepared according to the literature [30]. Other reagents were purchased from commercial sources without purification. A Perkin-Elmer 2400 CHN elemental analyzer was used to perform C, H, and N the elemental analyses. Infrared (IR) spectra of the two compounds were implemented with a Nicolet Impact 410 FTIR spectrometer (KBr pellet). Thermogravimetric (TG) analysis was carried out in flowing $N_2$ from 35°C to 900°C with a heating rate of 10°C min$^{-1}$ on a Diamond TG/DTA (Perkin-Elmer) thermal analyzer. Single-crystal XRD data of **1** and **2** were obtained from a Bruker Apex II CCD with Mo-K$\alpha$ radiation ($\lambda$ = 0.71073 Å) at 296 K using $\omega$–$2\theta$ scan method. The structures were solved by direct methods and refined by full-matrix least-squares on $F^2$ using SHELX-97 [31]. The crystal data and selected bond lengths and angles are listed in tables 1–3, respectively. Due to organic ligand disorder in **1**, some hydrogen atoms are not located.

Table 1. Crystal data for **1** and **2**.

| Compound | **1** | **2** |
|---|---|---|
| Empirical formula | $C_{24}H_{30}CoN_9O_{44}PW_{12}$ | $C_{48}H_{45}Mo_{12}N_{18}Ni_2O_{41.50}P$ |
| Formula weight | 3442.65 | 2837.69 |
| Temperature (K) | 296(2) | 296(2) |
| Wavelength (Å) | 0.71073 | 0.71073 |
| Crystal system | Rhombohedral | Triclinic |
| Space group | R-3c | $P\bar{1}$ |
| Unit cell dimensions (Å, °) | | |
| $a$ | 12.481(3) | 14.962(3) |
| $b$ | 12.481(3) | 17.311(3) |
| $c$ | 62.69(3) | 17.948(3) |
| $\alpha$ | | 79.407(2) |
| $\beta$ | | 73.806(2) |
| $\gamma$ | | 65.306(2) |
| Volume (Å$^3$), $Z$ | 8458(5), 6 | 4044.0(12), 2 |
| Calculated density (g cm$^{-3}$) | 4.055 | 2.330 |
| Absorption coefficient (mm$^{-1}$) | 24.795 | 2.366 |
| $F(000)$ | 9102 | 2732 |
| Crystal size (mm$^3$) | $0.15 \times 0.13 \times 0.12$ | $0.12 \times 0.10 \times 0.10$ |
| Limiting indices | $-14 \le h \le 15$;<br>$-14 \le k \le 15$;<br>$-77 \le l \le 77$ | $-17 \le h \le 18$;<br>$-20 \le k \le 20$;<br>$-21 \le l \le 19$ |
| Reflections collected | 19,263 | 29,102 |
| Independent reflection | 1839 [$R$(int) = 0.0527] | 14,599 [$R$(int) = 0.0590] |
| Max. and min. transmission | 0.1548 and 0.1185 | 0.7978 and 0.7644 |
| Refinement method | Full-matrix least-squares on $F^2$ | Full-matrix least-squares on $F^2$ |
| Data/parameters | 1839/174 | 14,599/1114 |
| Goodness-of-fit on $F^2$ | 1.022 | 1.007 |
| Final $R$ indices [$I > 2\sigma(I)$] | $R_1 = 0.0262$, $wR_2 = 0.0459$ | $R_1 = 0.0544$, $wR_2 = 0.1248$ |
| $R$ indices (all data) | $R_1 = 0.0503$, $wR_2 = 0.0492$ | $R_1 = 0.1184$, $wR_2 = 0.1463$ |

Table 2. Selected bond lengths (Å) and angles (°) for **1**.

| | | | |
|---|---|---|---|
| W(1)–O(4) | 1.651(6) | Co(1)–N(1)#4 | 1.941(6) |
| W(1)–O(2) | 1.877(5) | Co(1)–N(1)#5 | 1.941(6) |
| W(1)–O(5)#1 | 1.881(6) | Co(1)–N(1) | 1.941(6) |
| W(1)–O(5) | 1.896(6) | Co(1)–N(1)#6 | 1.940(6) |
| W(1)–O(3)#2 | 1.904(5) | Co(1)–N(1)#7 | 1.940(6) |
| W(1)–O(7) | 2.459(9) | Co(1)–N(1)#8 | 1.940(6) |
| W(1)–O(7)#2 | 2.463(9) | P(1)–O(7)#9 | 1.479(8) |
| W(2)–O(1) | 1.674(5) | P(1)–O(7) | 1.479(8) |
| W(2)–O(3) | 1.880(6) | P(1)–O(7)#3 | 1.479(8) |
| W(2)–O(8)#3 | 1.886(6) | P(1)–O(7)#10 | 1.479(8) |
| W(2)–O(8) | 1.901(6) | P(1)–O(7)#1 | 1.479(8) |
| W(2)–O(2) | 1.910(6) | P(1)–O(7)#2 | 1.479(8) |
| W(2)–O(9) | 2.434(7) | P(1)–O(9) | 1.596(12) |
| W(2)–O(7) | 2.590(8) | P(1)–O(9)#10 | 1.596(12) |
| N(1)#4–Co(1)–N(1)#5 | 92.6(3) | N(1)#6–Co(1)–N(1)#7 | 92.6(3) |
| N(1)#4–Co(1)–N(1)#6 | 81.9(4) | N(1)#4–Co(1)–N(1)#8 | 93.4(4) |
| N(1)#5–Co(1)–N(1)#6 | 93.4(4) | N(1)#5–Co(1)–N(1)#8 | 172.0(4) |
| N(1)–Co(1)–N(1)#6 | 172.0(4) | N(1)–Co(1)–N(1)#8 | 81.9(4) |
| N(1)#4–Co(1)–N(1)#7 | 172.0(4) | N(1)#6–Co(1)–N(1)#8 | 92.6(3) |
| N(1)#5–Co(1)–N(1)#7 | 81.9(4) | N(1)#7–Co(1)–N(1)#8 | 92.6(3) |
| N(1)–Co(1)–N(1)#7 | 93.4(4) | | |

Symmetry transformations used to generate equivalent atoms: #1 $x-y+1, x, -z$; #2 $y, -x+y+1, -z$; #3 $-y+2, x-y+1, z$; #4 $-y+1, x-y+1, z$; #5 $-x+y, -x+1, z$; #6 $y-1/3, x+1/3, -z-1/6$; #7 $-x+2/3, -x+y+1/3, -z-1/6$; #8 $x-y+2/3, -y+4/3, -z-1/6$; #9 $-x+y+1, -x+2, z$; #10 $-x+2, -y+2, -z$.

Table 3. Selected bond lengths (Å) and angles (°) for **2**.

| | | | |
|---|---|---|---|
| Mo(1)–O(29) | 1.683(4) | Mo(8)–O(32) | 1.909(4) |
| Mo(1)–O(2) | 1.838(4) | Mo(8)–O(36) | 1.932(4) |
| Mo(1)–O(7) | 1.851(4) | Mo(8)–O(11) | 1.957(4) |
| Mo(1)–O(19) | 1.961(4) | Mo(8)–O(1) | 2.422(4) |
| Mo(1)–O(3) | 2.006(4) | Mo(9)–O(21) | 1.684(4) |
| Mo(1)–O(6) | 2.431(3) | Mo(9)–O(15) | 1.794(4) |
| Mo(2)–O(12) | 1.683(4) | Mo(9)–O(3) | 1.898(4) |
| Mo(2)–O(20) | 1.857(4) | Mo(9)–O(35) | 1.928(4) |
| Mo(2)–O(23) | 1.868(4) | Mo(9)–O(30) | 2.041(4) |
| Mo(2)–O(16) | 1.929(4) | Mo(9)–O(6) | 2.419(4) |
| Mo(2)–O(17) | 1.979(4) | Mo(10)–O(37) | 1.673(4) |
| Mo(2)–O(18) | 2.430(3) | Mo(10)–O(40) | 1.848(4) |
| Mo(3)–O(8) | 1.691(4) | Mo(10)–O(19) | 1.866(4) |
| Mo(3)–O(9) | 1.824(4) | Mo(10)–O(33) | 1.990(4) |
| Mo(3)–O(4) | 1.898(3) | Mo(10)–O(31) | 2.014(4) |
| Mo(3)–O(16) | 1.928(4) | Mo(10)–O(5) | 2.442(4) |
| Mo(3)–O(39) | 2.009(4) | Mo(11)–O(28) | 1.708(4) |
| Mo(3)–O(18) | 2.438(3) | Mo(11)–O(22) | 1.933(4) |
| Mo(4)–O(27) | 1.683(4) | Mo(11)–O(4) | 1.934(4) |
| Mo(4)–O(30) | 1.828(4) | Mo(11)–O(38) | 1.935(4) |
| Mo(4)–O(26) | 1.835(4) | Mo(11)–O(33) | 1.943(4) |
| Mo(4)–O(23) | 1.999(4) | Mo(11)–O(5) | 2.406(4) |
| Mo(4)–O(7) | 2.018(4) | Mo(12)–O(25) | 1.724(4) |
| Mo(4)–O(6) | 2.465(4) | Mo(12)–O(11) | 1.864(4) |
| Mo(5)–O(24) | 1.653(4) | Mo(12)–O(38) | 1.884(4) |
| Mo(5)–O(34) | 1.831(4) | Mo(12)–O(40) | 2.019(4) |
| Mo(5)–O(17) | 1.831(4) | Mo(12)–O(15) | 2.022(4) |
| Mo(5)–O(36) | 1.969(4) | Mo(12)–O(5) | 2.428(4) |
| Mo(5)–O(26) | 2.003(3) | Ni(1)–N(8) | 2.022(5) |
| Mo(5)–O(1) | 2.460(4) | Ni(1)–N(6) | 2.039(5) |
| Mo(6)–O(14) | 1.692(4) | Ni(1)–N(2) | 2.058(4) |
| Mo(6)–O(31) | 1.824(4) | Ni(1)–N(7) | 2.089(5) |
| Mo(6)–O(39) | 1.832(3) | Ni(1)–N(1) | 2.125(4) |
| Mo(6)–O(2) | 1.988(4) | Ni(1)–N(5) | 2.155(5) |
| Mo(6)–O(20) | 1.993(4) | Ni(2)–N(14) | 2.012(6) |
| Mo(6)–O(18) | 2.452(4) | Ni(2)–N(10) | 2.063(6) |
| Mo(7)–O(13) | 1.690(3) | Ni(2)–N(15) | 2.071(5) |
| Mo(7)–O(22) | 1.853(4) | Ni(2)–N(13) | 2.130(5) |
| Mo(7)–O(32) | 1.900(4) | Ni(2)–N(11) | 2.155(7) |
| Mo(7)–O(9) | 1.979(4) | Ni(2)–N(12) | 2.173(6) |
| Mo(7)–O(34) | 1.993(4) | P(1)–O(1) | 1.518(4) |
| Mo(7)–O(1) | 2.463(3) | P(1)–O(6) | 1.529(3) |
| Mo(8)–O(10) | 1.697(4) | P(1)–O(18) | 1.530(4) |
| Mo(8)–O(35) | 1.903(3) | P(1)–O(5) | 1.534(4) |
| N(8)–Ni(1)–N(6) | 170.85(18) | N(14)–Ni(2)–N(10) | 90.7(2) |
| N(8)–Ni(1)–N(2) | 94.68(19) | N(14)–Ni(2)–N(15) | 94.4(2) |
| N(6)–Ni(1)–N(2) | 94.02(19) | N(10)–Ni(2)–N(15) | 171.7(3) |
| N(8)–Ni(1)–N(7) | 78.9(2) | N(14)–Ni(2)–N(13) | 167.5(2) |
| N(6)–Ni(1)–N(7) | 97.7(2) | N(10)–Ni(2)–N(13) | 79.5(2) |
| N(2)–Ni(1)–N(7) | 94.41(18) | N(15)–Ni(2)–N(13) | 96.2(2) |
| N(8)–Ni(1)–N(1) | 93.66(19) | N(14)–Ni(2)–N(11) | 79.6(2) |
| N(6)–Ni(1)–N(1) | 90.77(19) | N(10)–Ni(2)–N(11) | 94.9(2) |
| N(2)–Ni(1)–N(1) | 78.94(17) | N(15)–Ni(2)–N(11) | 92.4(2) |
| N(7)–Ni(1)–N(1) | 169.6(2) | N(13)–Ni(2)–N(11) | 93.3(2) |
| N(8)–Ni(1)–N(5) | 92.4(2) | N(14)–Ni(2)–N(12) | 92.2(2) |
| N(6)–Ni(1)–N(5) | 79.1(2) | N(10)–Ni(2)–N(12) | 95.2(2) |
| N(2)–Ni(1)–N(5) | 172.0(2) | N(15)–Ni(2)–N(12) | 78.1(2) |
| N(7)–Ni(1)–N(5) | 90.55(18) | N(13)–Ni(2)–N(12) | 96.4(2) |
| N(1)–Ni(1)–N(5) | 96.97(18) | N(11)–Ni(2)–N(12) | 167.1(2) |

### 2.2. *Syntheses*

**2.2.1. $[Co(pyim)_3][HPW_{12}O_{40}]\cdot 4H_2O$ (1).** A mixture of $Co(CH_3CO_2)_2\cdot 4H_2O$ (0.125 g, 0.5 mmol), $H_3[PW_{12}O_{40}]\cdot 12H_2O$ (0.450 g, 0.15 mmol), and 8 mL $H_2O$ was stirred for 2 h. The pH was adjusted to 4.0 with 6.0 mol$L^{-1}$ NaOH, then a solution prepared by dissolving 0.036 g 2-(2-pyridyl)-imidazole (0.25 mmol) into 4 mL $CH_3CH_2OH$ was added to the previous mixture, stirred 1 h, and transferred to a 25 mL Teflon-lined reactor and kept under autogenous pressure at 170°C for 5 days. Yellow cubic crystals were obtained (0.178 g, yield 35.58% based on W). Elemental Anal. Found (%): Co, 1.64; W, 63.27; C, 8.62; H, 0.79; N, 3.49 (Calcd (%): Co, 1.71; W, 64.08; C, 8.37; H, 0.88; N, 3.66).

**2.2.2. $[Ni(pyim)_3]_2[PMo^{V}Mo^{VI}_{11}O_{40}]\cdot 1.5H_2O$ (2).** The procedure of **2** was similar to that of **1** except that $Co(CH_3CO_2)_2\cdot 4H_2O$ and $H_3[PW_{12}O_{40}]\cdot 12H_2O$ were replaced by $Ni(CH_3CO_2)_2\cdot 4H_2O$ (0.125 g, 0.5 mmol) and $H_3[PMo_{12}O_{40}]\cdot 14H_2O$ (0.445 g, 0.21 mmol), respectively. Black cubic crystals were obtained (0.202 g, yield 33.23% based on Mo). Elemental Anal. Found (%): Ni, 4.05; Mo, 40.06; C, 20.43; H, 1.68; N, 8.65 (Calcd (%): Ni, 4.14; Mo, 40.57; C, 20.32; H, 1.60; N, 8.88).

### 2.3. *PXRD analyses*

PXRD measurements for **1** and **2** were carried out at room temperature. As shown in figure S1a (**1**) and figure S1b (**2**), the diffraction peak positions of simulated and experimental patterns match well, indicating the phase purity of **1** and **2**. Differences in reflection intensity are probably due to preferred orientation of the powder samples of **1** and **2** during collection of the experimental XRD data.

## 3. Results and discussion

### 3.1. *Crystal structure*

Compound **1** is constructed from $[HPW_{12}O_{40}]^{2-}$ and $[Co(pyim)_3]^{2+}$ and further connected by $(H_2O)_4$ clusters with hydrogen bonds to make the 3-D supermolecular framework. $[HPW_{12}O_{40}]^{2-}$ is the typical Keggin structure, in which W is six-coordinate to form $WO_6$ octahedra, and three $WO_6$ octahedra constitute a $W_3O_{13}$ trimer by edge-sharing and four $W_3O_{13}$ trimers connect by corner-sharing. The W–O and P–O bond lengths are 1.651(6)–2.590(8) Å and 1.479(8)–1.596(2) Å, respectively. These bond distances are comparable to the reported Keggin compounds [13, 17, 18]. Although many M–O cluster compounds based on $[PM_{12}O_{40}]^{n-}$ (M = W, Mo) have been reported [32–36], pyridyl imidazole combined with $[PM_{12}O_{40}]^{n-}$ has not been previously reported. As shown in figure 1, each Co is six-coordinate with six nitrogen atoms from three 2-(2-pyridyl)-imidazole molecules. The pyridine and imidazole rings of 2-(2-pyridyl)-imidazole are disordered with occupancy factors of 0.5 and 0.5. The Co–N bond lengths are between 1.940(6) and 1.941(6) Å. $(H_2O)_4$ water clusters (figure 2) link $[HPW_{12}O_{40}]^{2-}$ and $[Co(pyim)_3]^{2+}$ and are much different from reported water

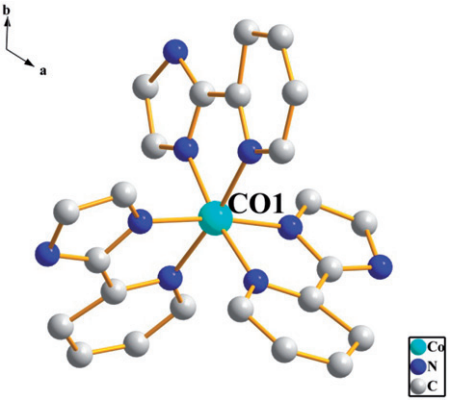


Figure 1. The crystal structure of $[Co(pyim)_3]^{2+}$ in **1** viewing along the *c*-axis.

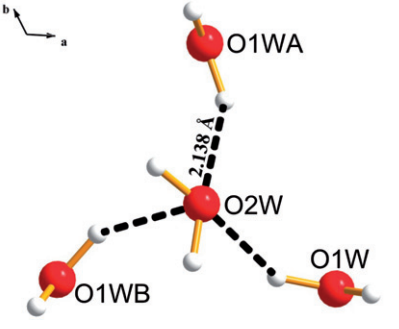


Figure 2. The $(H_2O)_4$ cluster in **1** viewed along the *c*-axis. Atoms with suffix A or B are generated by the symmetry operations: A, $2-y$, $2+x-y$, $z$; B, $-x+y$, $2-x$, $z$.

clusters [37–41]. The central $H_2O$ as H-acceptor connects the peripheral three water molecules by hydrogen bonds with O···O distance of 2.8136 Å (figure 2), and then $(H_2O)_4$ clusters connect organic ligands by hydrogen bonds to sheets with the three outer O1w as H-acceptors while connecting POMs with the three outer O1w as H-donors to other sheets. Occupancy factors of the disordered hydrogen atoms from the central $H_2O$ are 2/3. As shown in figure 3, each $(H_2O)_4$ connects three $[HPW_{12}O_{40}]^{2-}$ cages by hydrogen bonds to form a $\{[HPW_{12}O_{40}]\cdots(H_2O)_4\}_n$ layer, where the three outer O1w are H-donors with the O2···O1w distances being 2.9651(8) Å. Each $(H_2O)_4$ cluster links three $[Co(pyim)_3]^{2+}$ molecules by hydrogen bonds, with three outer O1w as H-acceptors with N···O distances of 2.6702 Å. Thus, the organic layers and inorganic layers are of staggered arrangement to form the supermolecular sandwich structure of **1** (figure 4).

In the structure of **2**, $[PMo^{V}Mo^{VI}_{11}O_{40}]^{4-}$ is also a Keggin structure with Mo–O distances varying from 1.653(4) Å to 2.465(4) Å. Two $[PMo^{V}Mo^{VI}_{11}O_{40}]^{4-}$ anions are connected by the van der Waals force with O28···O40 distance of 2.933 Å to form a "dipolymer" (figure 5). There are two kinds of $[Ni(pyim)_3]^{2+}$ cations, one three-connected with $[PMo^{V}Mo^{VI}_{11}O_{40}]^{4-}$ by N–H···O hydrogen bonds with N···O distances

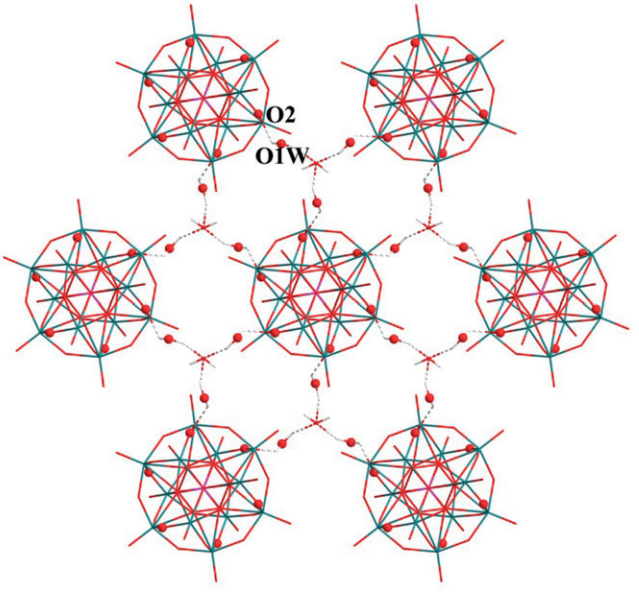


Figure 3. The structure of inorganic layer in **1** viewed along the *c*-axis.

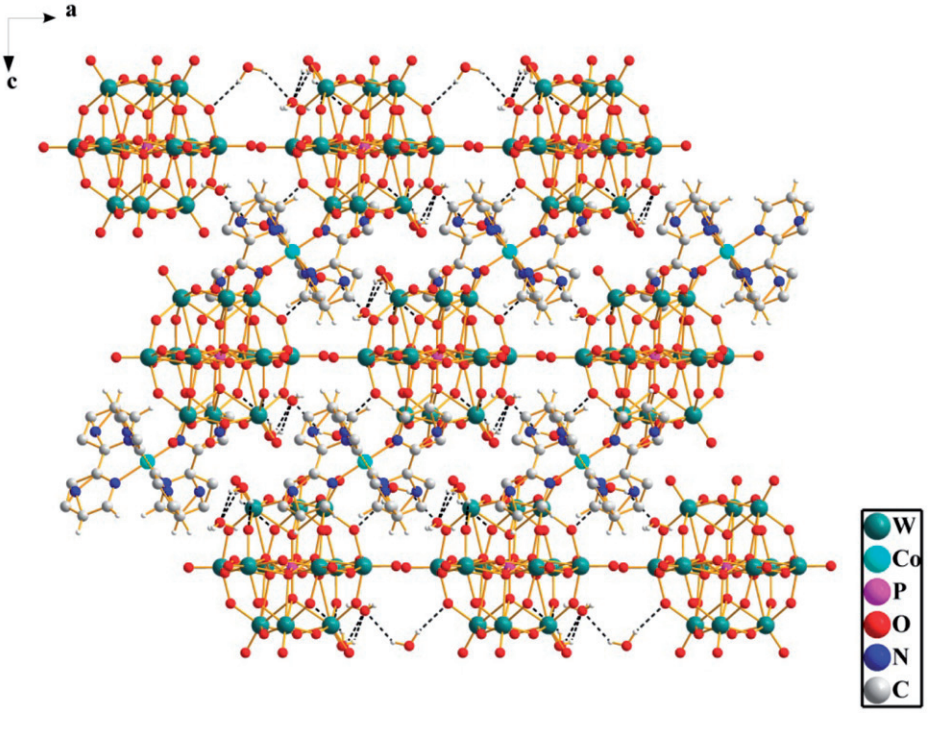


Figure 4. The 3-D supermolecular structure of **1**.

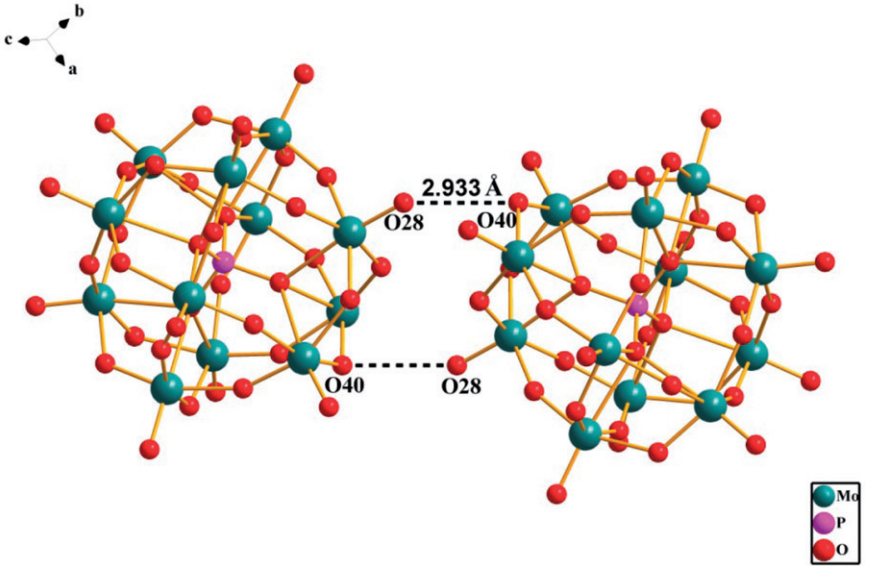


Figure 5. The "dipolymer" in **2**.

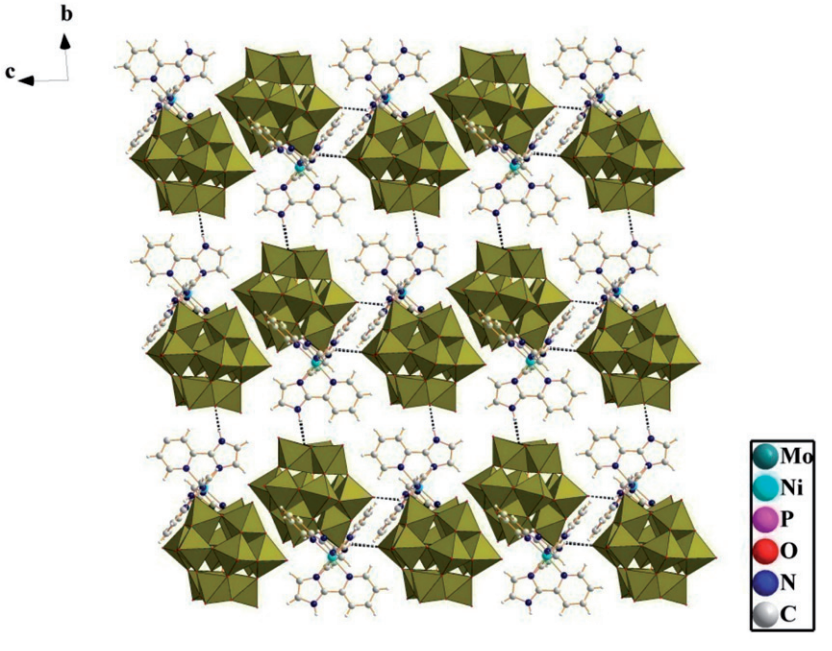


Figure 6. The supermolecular framework of **2**.

between 2.868(7) Å and 3.309(6) Å to form the supermolecular framework of **2** (figure 6) and the other two-connected with $[PMo^{V}Mo^{VI}_{11}O_{40}]^{4-}$ anions by N–H···O hydrogen bonds with N···O distances between 2.906(6) Å and 2.909(8) Å. As shown in figure 7, the topological net of **2** contains two kinds of nodes, purple nodes represent the

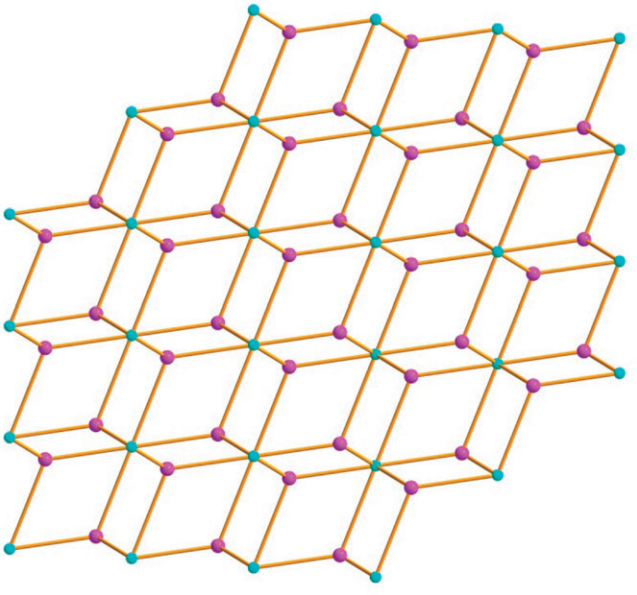

Figure 7. The topology net of **2** viewed along the *a*-axis. The three-connected nodes represent $[Ni(pyim)_3]^{2+}$ and the six-connected nodes represent $\{[PMo^{V}Mo^{VI}{}_{11}O_{40}]^{4-}\}_2$.

three-connected $[Ni(pyim)_3]^{2+}$ and blue nodes represent $\{[PMo^{V}Mo^{VI}_{11}O_{40}]^{4-}\}_2$; two-connected $[Ni(pyim)_3]^{2+}$ reside in the hollow space of the net. Bond valence sum calculations suggest one $Mo^{V}$ in **2**. The calculation results give values of 6.064 for Mo(1), 6.021 for Mo(2), 5.997 for Mo(3), 6.053 for Mo(4), 6.343 for Mo(5), 6.071 for Mo(6), 5.762 for Mo(7), 5.755 for Mo(8), 6.092 for Mo(9), 5.920 for Mo(10), 5.525 for Mo(11), and 5.402 for Mo(12) [42]; the average value is 5.917, in accord with the expected 5.917 for $[Mo^{V}_{1}Mo^{VI}_{11}]$.

### 3.2. *IR spectrum*

The IR spectrum of **1** (figure S2a) has sharp peaks at 1250–1650 $cm^{-1}$ typical of 2-(2-pyridyl)-imidazole. The peak at 1080 $cm^{-1}$ is ascribed to $\nu$(P–O). The strong band at 979 $cm^{-1}$ is due to $\nu$(W=O). Bands at 650–900 $cm^{-1}$ are associated with $\nu$(W–O–W). As shown in figure S2b, the IR spectrum of **2** is similar to that of **1**, 1250–1650 $cm^{-1}$ typical of 2-(2-pyridyl)-imidazole, 1053 $cm^{-1}$ and 951 $cm^{-1}$ due to $\nu$(P–O) and $\nu$(Mo=O) respectively, and 600–900 $cm^{-1}$ associated with $\nu$(Mo–O–Mo).

### 3.3. *Thermal analysis*

Thermal analysis of **1** from 25°C to 800°C (figure S3a) shows weight loss of 2.14% from 25°C to 200°C corresponding to loss of $H_2O$ (Calcd 2.09%). Weight loss of 12.18% from 200°C to 800°C can be attributed to the removal of pyim (Calcd 12.65%).

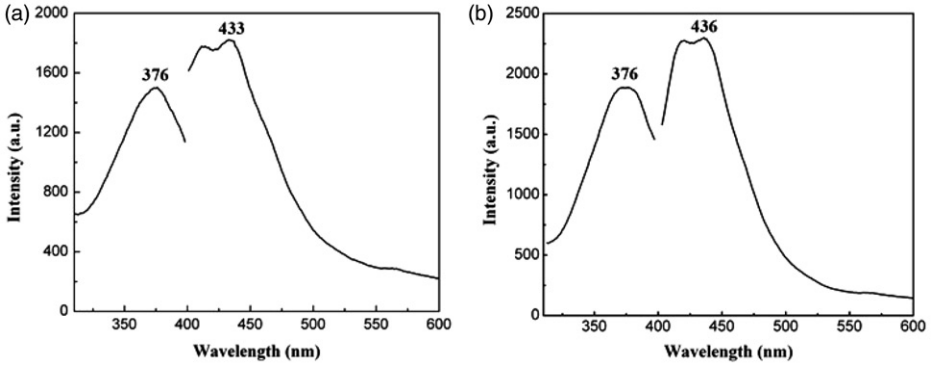


Figure 8. Excitation and emission spectra of **1**(a) and **2**(b).

The total weight loss of **2** (figure S3b) from 25°C to 800°C is 31.48% (Calcd 31.64%) due to the removal of $H_2O$ and pyim.

### 3.4. *Optical properties*

The fluorescence spectra of **1** and **2** recorded in solid at room temperature show (figure 8a) maximum excitation and emission wavelengths of **1** at 376 nm and 433 nm, respectively; maximum excitation and emission wavelengths of **2** (figure 8b) are 376 nm and 436 nm, respectively. Fluorescence of **1** and **2** are attributed to $[Co(pyim)_3]^{2+}$ and $[Ni(pyim)_3]^{2+}$. The maximum emission of **1** and **2** have a red-shift compared to free pyim (370 nm) [20], assigned to $\pi$–$\pi$* transition fluorescence and ligand-to-metal charge transfer [43–45]. The enhanced fluorescence efficiencies of **1** and **2** are attributed to coordination of pyim, effectively reducing loss of energy by radiationless thermal vibrations.

## 4. Conclusion

Two new organic–inorganic hybrid compounds based on POMs and pyridyl imidazole $[Co(pyim)_3][HPW_{12}O_{40}]\cdot 4H_2O$ (**1**) and $[Ni(pyim)_3]_2[PMo^{V}Mo^{VI}_{11}O_{40}]\cdot 1.5H_2O$ (**2**) have been hydrothermally synthesized. The synthesis of **1** and **2** indicates pyim can work with POMs to make new organic–inorganic hybrid compounds. Further work is in progress preparing other new organic–inorganic hybrid compounds based on POMs and pyim.

## Supplementary material

The supplementary crystallographic data for **1** and **2** with the deposited number CCDC Numbers 883860 and 883861 can be obtained free of charge

*via* http://www.ccdc.cam.ac.uk/conts/retrieving.html, or from Cambridge Crystallographic Data Centre, 12 Union Road, Cambridge CB2 1E2, UK; Fax: (+44) 1223-336-033; or E-mail: deposit@ccdc.cam.ac.uk

## Acknowledgements

This work was financially supported by the National Natural Science Foundation of China (20971068) and Jiangsu province (BK2012823).



## References

[1] P.D. Harvey, D. Fortin. *Coord. Chem. Rev*., **171**, 351 (1998).
[2] H.Y. An, E.B. Wang, D.R. Xiao, Y.G. Li, Z.M. Su, L. Xu. *Angew. Chem*., **118**, 918 (2006).
[3] F. Hussain, U. Kortz, B. Keita, L. Nadjo, M.T. Pope. *Inorg. Chem*., **45**, 761 (2006).
[4] C.T. Kresge, M.E. Leonowicz, W.J. Roth, J.C. Vartuli, J.S. Beck. *Nature*, **359**, 710 (1992).
[5] S. Kitagawa, R. Kitaura, S.I. Noro. *Angew. Chem. Int. Ed*., **43**, 2334 (2004).
[6] D. Maspoch, D. Ruiz-Molina, J. Veciana. *J. Mater. Chem*., **14**, 2713 (2004).
[7] U. Kortz, A. Muller, J.V. Slageren, J. Schnack, N.S. Dalal, M. Dressel. *Coord. Chem. Rev*., **253**, 2315 (2009).
[8] D.L. Long, E. Burkholder, L. Cronin. *Chem. Soc. Rev*., **36**, 105 (2007).
[9] A. Dolbecq, E. Dumas, C.R. Mayer, P. Mialane. *Chem. Rev*., **110**, 6009 (2010).
[10] D.L. Long, R. Tsunashima, L. Cronin. *Angew. Chem. Int. Ed*., **49**, 1736 (2010).
[11] C. Streb, C. Ritchie, D.L. Long, P. Kogerler, L. Cronin. *Angew. Chem. Int. Ed*., **46**, 7579 (2007).
[12] M.H. Rosnes, C. Musumeci, C.P. Pradeep, J.S. Mathieson, D.L. Long, Y.F. Song, B. Pignataro, R. Cogdell, L. Cronin. *J. Am. Chem. Soc*., **132**, 15 490 (2010).
[13] Z.G. Han, Y.L. Zhao, J. Peng, H.Y. Ma, Q. Liu, E.B. Wang. *J. Mol. Struct*., **738**, 1 (2005).
[14] Y. Xu, L.B. Nie, G.N. Zhang, Q. Chen, X.F. Zheng. *Inorg. Chem. Commun*., **9**, 329 (2006).
[15] C.Y. Duan, M.L. Wei, D. Guo, C. He, Q.J. Meng. *J. Am. Chem. Soc*., **132**, 3321 (2009).
[16] Q. Wu, X. Fu, J.W. Zhao, S.Z. Li, J.P. Wang, J.Y. Niu. *J. Coord. Chem*., **63**, 1844 (2010).
[17] B. Li, S.T. Zheng, G.Y. Yang. *Chin. J. Struct. Chem*., **28**, 531 (2009).
[18] M.G. Liu, P.P. Zhang, J. Peng, H.X. Meng, X. Wang, M. Zhu, D.D. Wang, C.L. Meng, K. Alimaje. *Cryst. Growth Des*., **12**, 1273 (2012).
[19] H.S. Liu, Y.Q. Lan, S.L. Li. *Cryst. Growth Des*., **10**, 5221 (2010).
[20] S.M. Yue, N. Li, J.Y. Bian, T.T. Hou, J.F. Ma. *Synth. Met*., **162**, 247 (2012).
[21] O. Schott, J. Ferrando-Soria, A. Bentama, S.E. Stiriba, J. Pasán, C. Ruiz-Pérez, M. Andruh, F. Lloret, M. Julve. *Inorg. Chim. Acta*, **376**, 358 (2011).
[22] J. Carranza, M. Julve, J. Sletten. *Inorg. Chim. Acta*, **361**, 2499 (2008).
[23] J. Carranza, J. Sletten, F. Lloret, M. Julve. *Polyhedron*, **28**, 2249 (2009).
[24] J. Carranza, J. Sletten, F. Lloret, M. Julve. *Inorg. Chim. Acta*, **362**, 2636 (2009).
[25] X. Yu, S. Cai, Z. Chen. *J. Inorg. Biochem*., **99**, 1945 (2005).
[26] G.X. Liu, Y.Y. Xu, R.Y. Huang, X.M. Ren. *Chin. J. Struct. Chem*., **26**, 1477 (2010).
[27] S.M. Yue, H.B. Xu, J.F. Ma, Z.M. Su, Y.H. Kan, H.J. Zhang. *Polyhedron*, **25**, 635 (2006).
[28] Y.Q. Lan, S.L. Li, Y.M. Fu, Y.H. Xu, L. Li, Z.M. Su, Q. Fu. *Dalton Trans*., 6796 (2008).
[29] H.Y. Zang, Y.Q. Lan, Z.M. Su, G.S. Yang, G.J. Xu, D.Y. Du, L. Chen, L.K. Yan. *Inorg. Chim. Acta*, **363**, 118 (2010).
[30] B. Chiswell, F. Lions, B. Morris. *Inorg. Chem*., **3**, 110 (1964).
[31] G.M. Sheldrick. SHE*LXTL version 5.10*, Bruker AXS Inc., Madison, WI (1997).
[32] M.L. Wei, H.H. Li, G.J. He. *J. Coord. Chem*., **64**, 4318 (2011).
[33] P. Shringarpure, B.K. Tripuramallu, K. Patel. *J. Coord. Chem*., **64**, 4016 (2011).
[34] Q.J. Kong, M.X. Hu, Y.G. Chen. *J. Coord. Chem*., **64**, 3237 (2011).
[35] H.N. Chen, Q. Wu, J.W. Zhao, S.Z. Li, J.P. Wang, J.Y. Niu. *J. Coord. Chem*., **63**, 1463 (2010).
[36] H.J. Pang, C.J. Zhang, Y.G. Chen, D.M. Shi. *J. Coord. Chem*., **63**, 418 (2010).
[37] H.Y. Liu, H.Y. Wang, Y.H. Shi. *J. Coord. Chem*., **64**, 2859 (2011).
[38] Y.N. Gong, C.B. Liu, X.H. Tang, A.Q. Zhang. *J. Coord. Chem*., **64**, 2761 (2011).
[39] S.K. Ghosh, J. Ribas, M.S.E. Fallah, P.K. Bharadwaj. *Inorg. Chem*., **44**, 3856 (2005).

[40] K.A. Siddiqui, G.K. Mehrotra, J. Mrozinski. *J. Coord. Chem.*, **64**, 2367 (2011).
[41] Z.P. Li, L. Huang, P.X. Xi, H.Y. Liu, Y.J. Shi, G.Q. Xie, M. Xu, F.J. Chen, Z.Z. Zeng. *J. Coord. Chem.*, **64**, 1885 (2011).
[42] I.D. Brown, M. O'Keeffe, A. Navrotsky. *Structure and Bonding in Crystals*, Vol. 2, Academic Press, New York, NY (1981).
[43] C.F. Zhong, R.F. Guo, Q. Wu, H.L. Zhang. *React. Funct. Polym.*, **67**, 408 (2007).
[44] S.G. Liu, J.L. Zuo, Y.Z. Li, X.Z. You. *J. Mol. Struct.*, **705**, 153 (2004).
[45] H. Wang, M.X. Li, M. Shao, X. He. *Polyhedron*, **26**, 5171 (2007).